

A Numerical Study on Electrophoresis of a Soft Particle with Charged Core Coated with Polyelectrolyte Layer

Partha Sarathi Majee, S. Bhattacharyya

Abstract—Migration of a core-shell soft particle under the influence of an external electric field in an electrolyte solution is studied numerically. The soft particle is coated with a positively charged polyelectrolyte layer (PEL) and the rigid core is having a uniform surface charge density. The Darcy-Brinkman extended Navier-Stokes equations are solved for the motion of the ionized fluid, the non-linear Nernst-Planck equations for the ion transport and the Poisson equation for the electric potential. A pressure correction based iterative algorithm is adopted for numerical computations. The effects of convection on double layer polarization (DLP) and diffusion dominated counter ions penetration are investigated for a wide range of Debye layer thickness, PEL fixed surface charge density, and permeability of the PEL. Our results show that when the Debye layer is in order of the particle size, the DLP effect is significant and produces a reduction in electrophoretic mobility. However, the double layer polarization effect is negligible for a thin Debye layer or low permeable cases. The point of zero mobility and the existence of mobility reversal depending on the electrolyte concentration are also presented.

Keywords—Debye length, double layer polarization, electrophoresis, mobility reversal, soft particle.

I. INTRODUCTION

SOFT particles or core-shell particles are very frequently encountered in biological matter such as proteins, DNA molecules and microorganisms, such as viruses or yeast cells [1]. The study of electrophoresis of a soft particle is of a great importance due to characterize their electrokinetic properties. The polymer coating of a nanoparticle is used to control colloidal stability, chemical functionality and dispersion rheology. The porous shell affects the electrophoretic mobility as the hydrodynamical and electrical forces are influenced by the shell [2]. A thin polyelectrolyte layer on the surface of a colloid can produce a vital effect on its electrophoretic mobility [3]. Soft particles has a vast use in pharmaceutical applications for the controlled release of drugs [4].

The electrophoresis of a spherical dispersion of soft particles was modeled by several investigators. An extensive theoretical studies dealing with the electrophoresis of soft particles has been provided by Ohshima [5]–[7]. In those studies, Ohshima has given analytical expressions for electrophoretic mobility of a soft particle with charged rigid core and uncharged shell, uncharged rigid inner core coated with charged polyelectrolyte

layer, or for a soft particle when both the core and shell are charged. Studies of Ohshima [5]–[7] are limited to weak applied electric field and it neglects the double layer polarization and relaxation effects. The theoretical analysis of Ohshima are verified experimentally by several authors e.g., López-Voita et al. [8]. Duval and Ohshima [9] in their study considered the soft particle coated with a diffuse polyelectrolyte in place of a uniformly distributed PEL by defining a gradual distribution of polymer segments within the permeable coating. Gopmandal et al. [10] extended the analytical expression of Ohshima [6] for the electrophoretic mobility of a charged soft particle with charged rigid core under a weak imposed field assumption.

The ion convection within the porous shell may not be negligible when the medium is highly permeable. It is established by several authors [3], [11]–[14] that at low ionic strength when the Debye layer is thicker than the porous coating, the double layer polarization and relaxation are important. The study of Hsu et al. [15] shows that the polarization effect is negligible when the rigid core of the soft particle have a low surface potential. Huang et al. [16] established that the mobility obtained under the coaxial Debye layer assumption overestimate the mobility obtained by considering the DLP effects. Zhang et al. [17] and Liu et al. [18] reviewed the impact of physical properties of the soft layer on the electrophoresis of a soft particle through a first-order perturbation analysis. The analysis of Yeh et al. [19] on soft particle shows that the mobility increase with the increase of bulk ionic concentration. The study of Chou et al. [20] shows that the influence of the porous layer on soft particles electrophoresis is significant when the double layer is thick. Cametti [14] in a review article analyzed the impact of the DLP and relaxation on electrophoresis of a soft particle. The effect of DLP and the influence of boundary shape on the electrophoresis of soft spherical particle has been studied numerically by Tseng et al. [21]. In those studies the DLP effect is taken into account through a first order perturbation from the equilibrium Boltzmann distribution under an weak applied field assumption. Barbati and Kirby [22] suggested that a numerical method must be approached to analyze the electrokinetics of a soft particle when the soft polymer layer thickness is not larger than the Debye layer of the rigid core. Raafatnia et al. [23] studied the electrophoresis of a negative colloid grafted with positive polyelectrolyte by presenting a molecular dynamics simulation and described the occurrence of mobility reversal in a monovalent electrolyte solution.

S. Bhattacharyya is with the Department of Mathematics, Indian Institute of Technology Kharagpur, Kharagpur-721302 (corresponding author, e-mail: somnath@maths.iitkgp.ernet.in).

Partha Sarathi Majee is with the Department of Mathematics, Indian Institute of Technology Kharagpur, Kharagpur-721302 (e-mail: psmajee5@gmail.com).

Bhattacharyya and De [24] made a numerical investigation of the electrophoresis of a soft particle with uncharged dielectric core in presence of a non-weak electric field and shown the impact of the DLP. Recently, De et al. [25] have analyzed numerically the electrophoresis of a soft particle with dielectric rigid core possessing a constant volumetric charge density.

In the present article, we performed a numerical investigation on the electrophoresis of a soft particle with charged rigid core and coated with a charged polyelectrolyte layer immersed in an unbounded electrolyte without considering any limitation on the external electric field, charged density of the PEL or Debye layer thickness. For a non-weak applied field or when the charge density of the PEL is not low enough, analytic solutions or solutions based on first-order perturbation analysis are may not appropriate. Considering the rigid core charged negatively and the polyelectrolyte charged positively, we presented the occurrence of zero electrophoretic mobility and mobility reversal by varying the electrolyte concentration.

II. MATHEMATICAL MODEL

We consider the electrophoresis of a soft spherical particle of radius b with a charged rigid core of radius a , coated with a polyelectrolyte layer (PEL) of thickness $(b - a)$ in a symmetric electrolyte solution. The particle is moving with electrophoretic velocity U_E^* in response to an applied electric field E_0 . The electric permittivity ϵ_e of the polymer layer is taken to be same that of the electrolyte and the PEL is assumed as Brinkman porous medium with screening length ℓ bearing a constant fixed charge density ρ_f . The spherical polar coordinate system (r, θ, ψ) is adopted with its origin fixed at the center of the particle and z -axis ($\theta = 0$) is along the imposed field E_0 (Fig. 1). We assume that the problem is axially symmetric with z -axis as the axis of symmetry.

The equations governing the motion of the ionized fluid inside the PEL are Darcy-Brinkman extended Navier-Stokes equation and in the electrolyte are Navier-Stokes equation. We considered the Nernst-Planck equations for the transport of ions. The electric field in the soft layer and in the electrolyte is governed by the Poisson equation. We scale the dimensional variables as follows: the radius of the soft sphere b is the length scale, the thermal potential $\phi_0 = k_B T / e$ is the potential scale, $U_0 = \epsilon_e \phi_0^2 / b \mu$ is the velocity scale, $\tau = b / U_0$ is the time scale, $\epsilon_e \phi_0^2 / b^2$ is the pressure scale, the bulk ionic concentration n_0 is the scale for the ion concentration of the i^{th} ionic species and $\Lambda = E_0 b / \phi_0$ is the scaled external electric field. Here e is the elementary charge, k_B is the Boltzmann constant, T is the absolute temperature and μ is the dynamic viscosity. We define $e_p = (1 - \gamma)$ as the non-dimensional PEL thickness, where $\gamma = a/b$ is the scaled core radius.

The equations of Newtonian incompressible fluid describing the motion of ionized fluid inside the PEL and outside the soft layer can be expressed in non-dimensional form as,

$$Re \frac{\partial \mathbf{u}}{\partial t} - \nabla^2 \mathbf{u} + \nabla p + B \beta^2 \mathbf{u} + \frac{(\kappa a)^2}{2} \rho_e \nabla \phi = 0 \quad (1)$$

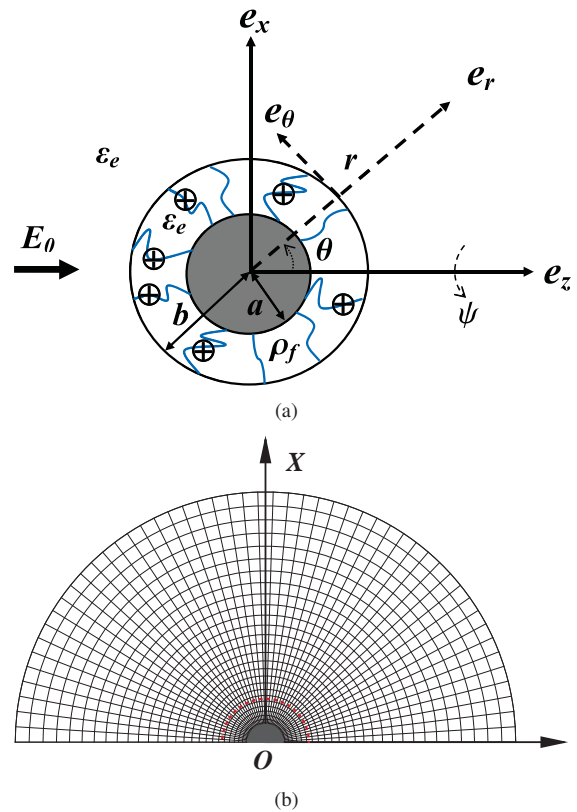


Fig. 1 (a) Schematic description of the geometry and the spherical coordinate system; (b) Grid distribution inside and around the soft particle: The red dashed line represents the surface of the soft particle

$$\nabla \mathbf{u} = 0 \quad (2)$$

where $\mathbf{u} = (u, v)$ is the velocity vector, v is the radial and u is the cross radial velocity components, t is the time, p is the pressure, ϕ is the electrical potential and $\rho_e = (n_1 - n_2)$ is the charged density with $n_i (i = 1, 2)$ is the ionic concentration of the i^{th} ionic species with valence $z_i = \pm \mathcal{Z}$. Here $Re = U_0 a \rho / \mu$ is the Reynolds number, ρ is the fluid density and $\kappa = \sqrt{2 \mathcal{Z} e n_0 / \epsilon_e \phi_0}$ is the inverse of the EDL thickness. The non-dimensional parameter $\beta = a / \ell$ determines the permeability of the PEL and the binary parameter $B = 1$ inside the soft layer ($\gamma < r < 1$) and $B = 0$ in the electrolyte medium ($r > 1$).

The non-dimensional Nernst-Planck equation governing the distribution of the i^{th} ionic species is

$$Pe_i \frac{\partial n_i}{\partial t} + Pe_i (\mathbf{u} \cdot \nabla n_i) = \nabla^2 n_i + \frac{z_i}{\mathcal{Z}} \nabla \cdot (n_i \nabla \phi) \quad (3)$$

where D_i is the diffusivity of the i^{th} ion with that the non-dimensional parameter $Pe_i = \epsilon_e \phi_0^2 / \mu D_i$, measures the ratio of advective to diffusion transport of ions.

The electric potential is governed by the Poisson equation

$$\nabla^2 \phi = - \frac{(\kappa b)^2}{2} \rho_e - B Q_f \quad (4)$$

where $Q_f = \rho_f b^2 / \epsilon_e \phi_0$ is the scaled fixed charged density of the PEL.

A no-slip boundary condition and no normal flux of ions are imposed on the surface of the particle ($r = \gamma$)

$$\mathbf{u} = 0, \quad [\nabla n_i + (z_i/Z) n_i \nabla \phi] \cdot \mathbf{e}_r = 0 \quad (5)$$

Here \mathbf{e}_r is unit vector along the radial direction.

The jump in the electric displacement on the surface of the particle ($r = \gamma$) is related to surface charged density as

$$\frac{\partial \phi}{\partial r} = -\sigma \quad (6)$$

where σ is the surface charge density on the core and is scaled by $\varepsilon_e \phi_0 / b$.

Far from the particle ($r \rightarrow \infty$)

$$\mathbf{u} = -U_E \mathbf{e}_z, \quad \phi = -\Lambda r \cos \theta, \quad n_i = 1 \quad (7)$$

The non-dimensional electrophoretic velocity U_E scaled by U_0 is unknown a priori, it is obtained iteratively by solving the balance of electrical and hydrodynamical forces. The mobility of the particle is defined as $\mu_{E^*} = U_E^* / E_0$. The non-dimensional mobility μ_E is obtained by scaling μ_{E^*} with $\varepsilon_e \phi_0 / \mu$.

The forces experienced by the soft particle are the electric force and drag force. The axisymmetric nature of our problem suggests that only the z -component of these forces need to be considered. The electrostatic and hydrodynamic forces along the flow direction can be calculated by integrating the Maxwell stress tensor σ^E and hydrodynamic stress tensor σ^H respectively, on the surface of the soft particle and are given by

$$F_E^* = \iint_S (\sigma^E \cdot \mathbf{e}_r) \cdot \mathbf{e}_z dS \quad (8)$$

$$F_D^* = \iint_S (\sigma^H \cdot \mathbf{e}_r) \cdot \mathbf{e}_z dS \quad (9)$$

where $\sigma^E = \varepsilon_e [\mathbf{E}\mathbf{E} - (1/2)E^2 \mathbf{I}]$ and $\sigma^H = -p\mathbf{I} + \mu[\nabla \mathbf{u} + (\nabla \mathbf{u})^T]$. Here $\mathbf{E} = -\nabla \phi$, $E^2 = \mathbf{E} \cdot \mathbf{E}$, $\mathbf{E}\mathbf{E}$ denotes the vector direct product and \mathbf{I} is the unit tensor. The variables with an asterisks in superscript denote the dimensional quantities.

$$F_E = - \iint_S \left[\frac{\partial \phi}{\partial r} \frac{\partial \phi}{\partial z} - \frac{1}{2} \left\{ \left(\frac{\partial \phi}{\partial r} \right)^2 + \left(\frac{1}{r} \frac{\partial \phi}{\partial \theta} \right)^2 \right\} \cos \theta \right] dS \quad (10)$$

$$F_D = \iint_S \left[\left\{ -p + 2 \frac{\partial v}{\partial r} \right\} \cos \theta - \left\{ \frac{\partial}{\partial r} \left(\frac{u}{r} \right) + \frac{1}{r} \frac{\partial v}{\partial \theta} \right\} \sin \theta \right] dS \quad (11)$$

The forces F_E and F_D are scaled by $\varepsilon_e \phi_0^2$.

The electrophoretic velocity U_E is determined through the force balance equation $F_E + F_D = 0$ iteratively. The forces are obtained by solving the governing electrokinetic equations through the numerical method as outlined in the following section.

III. NUMERICAL METHODS

The coupled governing equations for ion transport, fluid flow, and electric potential along with the provided boundary conditions are solved numerically over a staggered grid system using a control volume method. In a staggered grid system, the velocity components are stored at the midpoints of the cell side normal to their direction while the scalar quantities are taken at the center of the cells. The governing equations are discretized by integrating them over each control volume. A pressure correction based iterative SIMPLE(Semi-Implicit Method for Pressure-Linked Equations) algorithm is adopted to solve the coupled non-linear equations. The solution is made through a cyclic guess-and-correct procedure. The pressure link between the continuity and momentum equations are performed by converting the discretized continuity equation into a Poisson equation for correction of pressure. This Poisson equation implements a pressure correction for a divergent velocity field. At each iteration, the equation for the electric field i.e., (4) is solved through the Successive-Over-Relaxation technique.

A time-dependent numerical solution is achieved by advancing the variables through a sequence of short time steps. We start the motion from the initial stationary condition and achieve a steady-state after a large time step for which the variables become independent of time. In order to validate the accuracy of our algorithm, we compared our results with the existing analytical solution which is explained in the next section.

IV. RESULTS AND DISCUSSION

In the present investigation, we have taken $\phi_0 = 0.02586$ V, $\varepsilon_e = 695.39 \times 10^{-12}$ C/Vm, $\mu = 10^{-3}$ Pa.s, $\rho = 10^3$ kg/m³, $b = 100$ nm, $D_1 = 1.33 \times 10^{-9}$ m²/s and $D_2 = 2.03 \times 10^{-9}$ m²/s.

To make a comparison of the present computations with the analytical solution, variation of electrophoretic mobility with Debye length and the corresponding analytical results due to Ohshima [6] are presented in Fig. 2 (a) when the rigid core of the particle is uncharged ($\sigma = 0$). In Fig. 2 (b), we present the electrophoretic mobility of the particle with uncharged PEL ($\rho_f = 0$). Electrophoretic mobility due to the analytic expression of Ohshima [5] for a fixed ζ -potential is also presented in Fig. 2 (b) by transforming σ to corresponding ζ based on the relation $\zeta = 2 \sinh^{-1}(\sigma/\kappa b)$ for thin Debye layer. One can note that, Ohshima [5], [6] in his studies did not account the relaxation and DLP effects. Whereas the present model consider the double layer polarization by convection and electromigration of ions and relaxation by the molecular diffusion of ions. Fig. 2 (a) shows that, our results are overestimated by the analytic solution of Ohshima [6] for higher values of PEL fixed charge density at low κb as the DLP effect might be strong. Our results approach to the analytic results due to Ohshima [6] when the Debye layer is thin. Our computed mobility of the particle with uncharged PEL are also in a good agreement with Ohshima [5] for thin Debye layer.

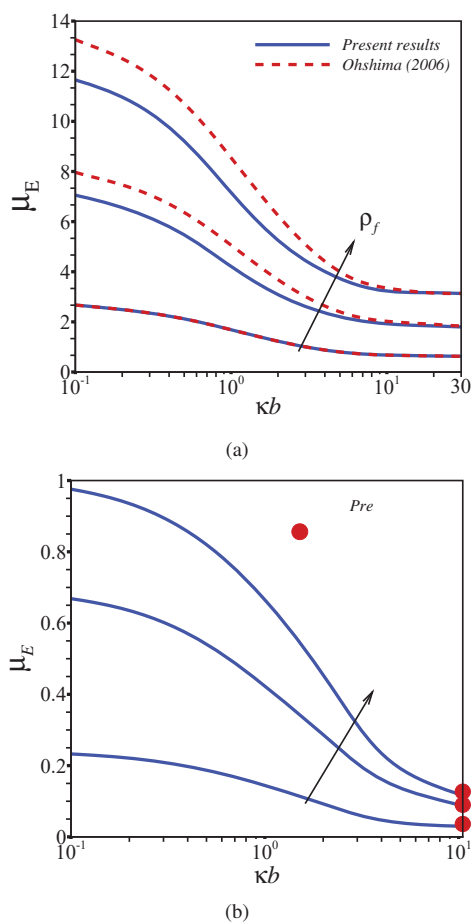


Fig. 2 Variation of electrophoretic mobility μ_E with κb for (a) different $\rho_f = [1.8, 3.6, 5.4] \times 10^4 \text{ Cm}^{-3}$ with $\sigma = 0$ and (b) different $\sigma = [1.8, 5.4, 9] \times 10^{-4} \text{ Cm}^{-2}$ with $\rho_f = 0$; when $\beta = 3$, $e_p = 0.5$ and $\Lambda = 1$. Red dashed lines in Fig. 2 (a) represent the corresponding analytical results due to Ohshima [6]. Symbols in Fig. 2 (b) denotes the mobility due to Ohshima [5] with scaled surface potential, $\zeta=0.1,0.3,0.4$ based on the relation $\sigma = 2\kappa b \sinh(\zeta/2)$

In the present study, we have analyzed the variation of our computed mobility along with a superposed mobility of the particle with charged core coated with charged PEL as a function of the key parameters such as Debye length, PEL thickness and softness parameter (β). We determine the superposed mobility (μ_E^S) through a linear superposition of the mobility ($\mu_E|_{\sigma=0}$) of the particle with uncharged core and charged PEL with the mobility ($\mu_E|_{\rho_f=0}$) of the particle with charged core and uncharged PEL i.e., $\mu_E^S = \mu_E|_{\sigma=0} + \mu_E|_{\rho_f=0}$. Throughout the paper, we carried out a comparative study between the computed and superposed mobility of the particle.

The variation of computed and superposed mobility with the Debye length at different values of PEL fixed charged density and core surface charge density is illustrated in Figs. 3 (a) and (b). A large discrepancy is observed between the computed and superposed mobility values for larger values of fixed PEL charged density when the Debye length is in the order of the particle size, i.e., $\kappa b \sim O(1)$. In this situation, the superposed mobility underestimates the computed mobility. The deviation increase as the ρ_f and surface charge density of the core become higher. Computed mobility merges with

the mobility based on the linear superposition technique when the Debye layer thickness is thin and fixed charged density of the shell is low. When the Debye layer is thick and the fixed charged density of the PEL is high, the electroosmotic flow (EOF) within the polyelectrolyte is strong and it drags the counterions towards the negative z -axis. A deformation in the distribution of counterions in the double layer can be observed which creates an induced electric field. This induced electric field is strong when the Debye length is thick. The superposition principle fails to account this interaction of EOF with the double layer. This might be the possible cause for the superposed mobility to underestimate the computed mobility for a thick double layer. For low fixed charge density of the PEL and the double layer is thin, the EOF is low and the DLP effect is negligible and therefore the the mobility based on the superposition principle agree well with the computed mobility values.

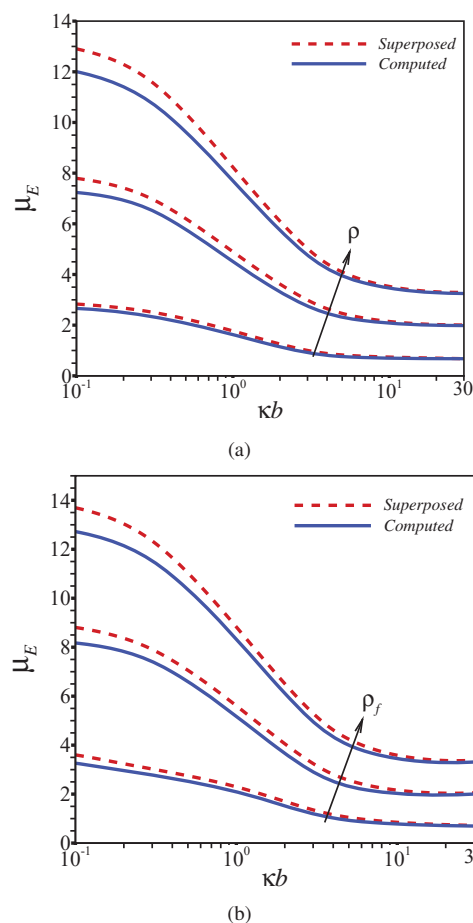


Fig. 3 Variation of electrophoretic mobility μ_E with κb for (a) $\sigma = 1.8 \times 10^{-4} \text{ Cm}^{-2}$ and (b) $\sigma = 9 \times 10^{-4} \text{ Cm}^{-2}$; with different $\rho_f (= [1.8, 3.6, 5.4] \times 10^4 \text{ Cm}^{-3})$ when $\beta = 3.0$, $e_p = 0.5$, $\Lambda = 1$. Here solid lines represent computed mobility values and dashed lines represent superposed ($\mu_E|_{\sigma=0} + \mu_E|_{\rho_f=0}$) mobility values

Figs. 4 (a) and (b) represent the variation of computed and superposed electrophoretic mobility with polyelectrolyte layer thickness (e_p) for different range of fixed charged density of the PEL and for different surface charge density of the rigid core when the double layer thickness is same

as the particle radius i.e, $\kappa b = 1$. We observed that the computed electrophoretic mobility differs from the superposed mobility when the porous layer thickness is low and the fixed charged density of the PEL is higher. The computed results merge with the superposed results as e_p grows. The polarization effect is significant when the double layer extends beyond the polyelectrolyte layer which corresponds to a smaller value of e_p . The double layer polarization creates an induced electric field due to the re-distribution of counterions in the diffuse layer which act against the imposed electric field. The effect of the electroosmotic flow governed by the counterions in the Debye layer is strong for a thinner porous layer. The interaction of this EOF with the induced electric field generated by the DLP can be a reason for the deviation of the computed electrophoretic mobility from the superposed electrophoretic mobility. For higher values of the PEL fixed charge density, the interaction of the electroosmotic flow, counterion condensation and double layer polarization becomes strong. When the porous layer thickness is large, the distribution of the ions are dominated by the diffusion and the DLP effect is negligible. The thick polyelectrolyte layer decreases the effect of the rigid core charge density and also screens the EOF.

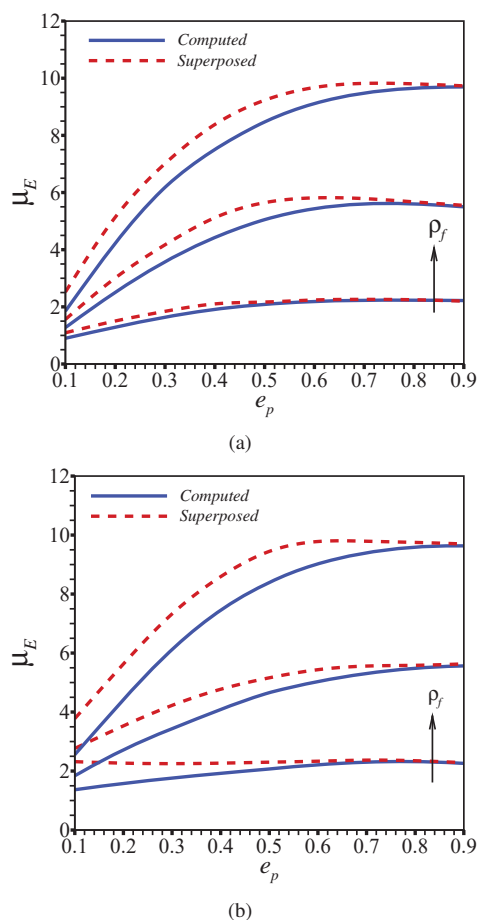


Fig. 4 Variation of electrophoretic mobility μ_E with soft layer thickness e_p for (a) $\sigma = 1.8 \times 10^{-4} \text{ Cm}^{-2}$ and (b) $\sigma = 9 \times 10^{-4} \text{ Cm}^{-2}$; with different ρ_f ($= [1.8, 3.6, 5.4] \times 10^4 \text{ Cm}^{-3}$) when $\kappa b = 1$, $\beta = 3.0$, $\Lambda = 1$. Here solid lines represent computed mobility values and dashed lines represent superposed ($\mu_E|_{\sigma=0} + \mu_E|_{\rho_f=0}$) mobility values

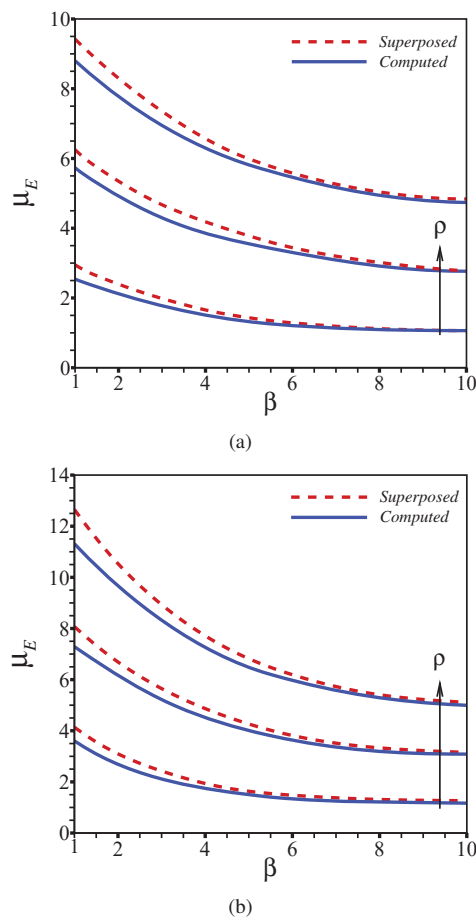


Fig. 5 Variation of electrophoretic mobility μ_E with β for (a) $\sigma = 1.8 \times 10^{-4} \text{ Cm}^{-2}$, (b) $\sigma = 5.4 \times 10^{-4} \text{ Cm}^{-2}$ and (c) $\sigma = 9 \times 10^{-4} \text{ Cm}^{-2}$; with different ρ_f ($= [1.8, 3.6, 5.4] \times 10^4 \text{ Cm}^{-3}$) when $\kappa b = 1$, $e_p = 0.5$, $\Lambda = 1$. Here solid lines represent computed mobility values and dashed lines represent superposed ($\mu_E|_{\sigma=0} + \mu_E|_{\rho_f=0}$) mobility values

Variation of the computed and superposed electrophoretic mobility with the softness parameter β is depicted in Figs. 5 (a) and (b) for different values of PEL fixed charged density and core surface charge density. We find that the computed electrophoretic mobility deviates from the electrophoretic mobility based on the superposition technique for high permeable case (low β). For a high permeable polyelectrolyte layer the polarization effect is significant. When the porous layer becomes more dense i.e, β increases the electrophoresis is dominated by the PEL. The effect of the surface charge density of the rigid core is reduced at high β as the electroosmotic flow induced by the core is suppressed by the low permeable soft layer. The DLP effect is very low for higher value of β and therefore no difference is observed between the computed and electrophoretic mobility.

The distribution of counterions and stream lines around the soft particle is shown in the Fig. 6 (a) at $\kappa b = 1$. Fig. 6 (b) shows the distribution of net ionic concentration around the particle. A deformation of double layer near the particle is evident from the figures. A Stokes flow around the particle is observed from the streamlines patterns. The contours show a counterion plum occurs along the downstream of the particle.

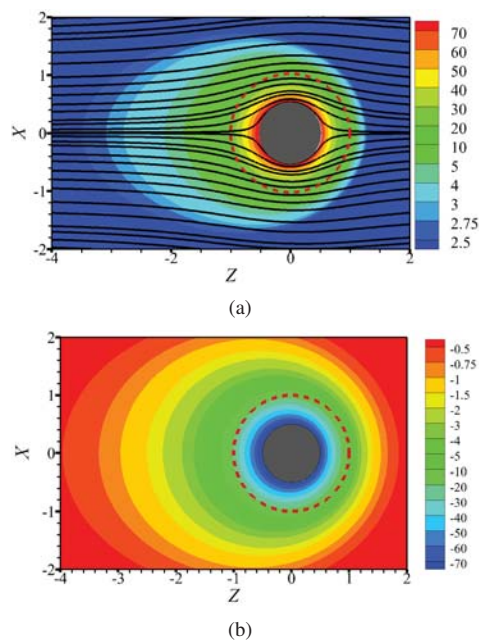


Fig. 6 (a) Stream lines and counterion distribution; and (b) net ionic concentration for $\rho_f = 5.4 \times 10^4 \text{ Cm}^{-3}$, $\sigma = 9 \times 10^{-4} \text{ Cm}^{-2}$, $\kappa b = 1$, $e_p = 0.5$, $\beta = 1$ and $\Lambda = 1$. Red dashed lines represents the outer surface of the soft particle

In Fig. 7, we estimate the critical surface charge density of the rigid core as a function of the fixed charge density of the PEL for which the electrophoretic mobility of the particle becomes zero. We present this critical σ or the point of zero mobility (PZM) for different values of κb . Studies of Moussa [26] for electrophoresis of a nano dendrimer with oppositely charged inner and outer soft shells reports a strong dependency of the PZM on electrolyte concentration. The results are presented for a highly permeable polyelectrolyte layer and when the soft layer thickness $e_p = 0.25$. It is evident from the figure that the critical value of σ corresponding to a fixed charge density of the PEL increase with the increase of electrolyte concentration.

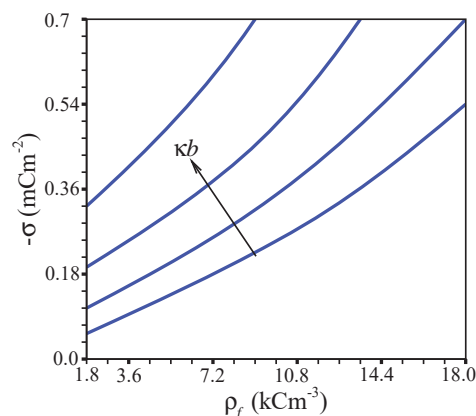


Fig. 7 Critical value of core surface charge density σ as a function of PEL fixed charge density ρ_f for different κb ($= 0.1, 1, 5, 10$) when $\beta = 1$, $e_p = 0.25$ and $\Lambda = 1$

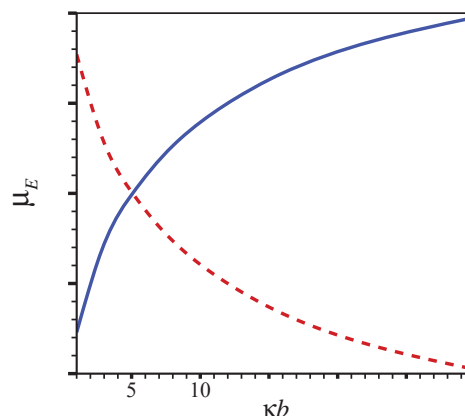


Fig. 8 Variation of electrophoretic mobility with κb when $\rho_f = 1.8 \times 10^4 \text{ Cm}^{-3}$, $\sigma = -7.2 \times 10^{-4} \text{ Cm}^{-2}$ (solid lines) and $\rho_f = -1.8 \times 10^4 \text{ Cm}^{-3}$, $\sigma = 7.2 \times 10^{-4} \text{ Cm}^{-2}$ (dashed line) when $\beta = 1$, $e_p = 0.25$ and $\Lambda = 1$

Electrophoresis of a soft particle is governed by both the core surface charge and PEL charge density for a low to a moderate value of double layer thickness. When the double layer around the rigid core expands beyond the PEL thickness the impact of the core surface charge density decreases and the electrophoresis is started being dominated by the PEL charge. We illustrate the variation of the electrophoretic velocity of the particle with Debye length when the polyelectrolyte layer and the rigid core are oppositely charged in Fig. 8. For a positively (negatively) charged core and negatively (positively) charged PEL the particle velocity switches from a positive (negative) value to a negative (positive) value as the Debye layer exceeds the PEL thickness. A similar kind of observation was made by De et al. [25] for a soft particle with a rigid core having a volumetric charge density. For a higher ionic concentration, the PEL charge density determines the particle velocity.

V. CONCLUSION

We have investigated the electrophoresis of a soft particle with charged core coated with a polyelectrolyte layer. We have performed numerical simulations of the coupled Navier-Stokes-Nernst-Planck equations to account perfectly the impact of molecular diffusion, electromigration, and ion advection. Considering the DLP and relaxation effect, electrophoresis of a soft particle has been studied by comparing our computed results with the results based on a superposition principle. Our results show that the results based on the superposition technique underestimate the computed results for a thick Debye layer, thin PEL layer or for a high permeable shell due to the strong DLP effect. When the Debye length becomes thinner the superposed electrophoretic mobility merges with the computed electrophoretic mobility. A zero electrophoretic velocity is estimated for different Debye layer by considering oppositely charged core and PEL.

REFERENCES

- [1] JFL. Duval, and F. Gaboriaud, *Progress in electrohydrodynamics of soft microbial particle interphases*, Current Opinion in Colloid & Interface Science, 15(3):184-195,2010.

- [2] X. Yang, S. Lin, and MR. Wiesner, *Influence of natural organic matter on transport and retention of polymer coated silver nanoparticles in porous media*, Journal of hazardous materials, 264:161-168,2014.
- [3] DA. Saville, *Electrokinetic properties of fuzzy colloidal particles*, Journal of colloid and interface science, 222(1):137-145,2000.
- [4] X. Yang, S. Lin, and MR. Wiesner, *Electrosprayed core-shell nanoparticles of PVP and shellac for furnishing biphasic controlled release of ferulic acid*, Colloid and Polymer Science, 292(9):2089-2096,2014.
- [5] H. Ohshima, *Modified Henry function for the electrophoretic mobility of a charged spherical colloidal particle covered with an ion-penetrable uncharged polymer layer*, Journal of Colloid and Interface Science, 252(1):119-125,2002.
- [6] H. Ohshima, *Electrophoresis of soft particles: Analytic approximations*, Electrophoresis, 27(3):526-533,2006.
- [7] H. Ohshima, *Electrokinetic phenomena of soft particles*, Current Opinion in Colloid & Interface Science, 18(2):73-82,2013.
- [8] J. López-Voitá, S. Mandal, A.V. Delgado, J.L. Toca-Herrera, M. Möller, F. Zanuttin, M. Balestrino and S. Krol, *Electrophoretic characterization of gold nanoparticles functionalized with human serum albumin (HSA) and creatine*, Journal of Colloid and Interface Science, 332(1):215-223,2009.
- [9] JFL. Duval, and H. Ohshima *Electrophoresis of diffuse soft particles*, Langmuir, 22(8):3533-3546,2006.
- [10] PP. Gopmandal, S. Bhattacharyya, and H. Ohshima *Effect of core charge density on the electrophoresis of a soft particle coated with polyelectrolyte layer*, Colloid and Polymer Science, 294(4):727-733,2016.
- [11] RJ. Hill and DA. Saville, *Exact solutions of the full electrokinetic model for soft spherical colloids: Electrophoretic mobility*, Colloids and Surfaces A: Physicochemical and Engineering Aspects, 267(1):31-49,2005.
- [12] RJ. Hill, DA. Saville, and WB. Russel, *Electrophoresis of spherical polymer-coated colloidal particles*, Journal of Colloid and Interface Science, 258(1):56-74,2003.
- [13] JJ. López-García, C. Grosse, and J. Horno, *Numerical study of colloidal suspensions of soft spherical particles using the network method: I. DC electrophoretic mobility*, Journal of colloid and interface science, 265(2):327-340,2003.
- [14] C. Cametti, *Dielectric properties of soft-particles in aqueous solutions*, Soft Matter, 7(12):5494-5506,2011.
- [15] JP. Hsu, ZS. Chen, and S. Tseng, *Effect of electroosmotic flow on the electrophoresis of a membrane-coated sphere along the axis of a cylindrical pore*, The Journal of Physical Chemistry B, 113(21):7701-7708,2009.
- [16] S. Tseng, JP. Hsu, HM. Lo, and LH. Yeh, *Electrophoresis of a Soft Particle within a Cylindrical Pore: Polarization Effect with the Nonlinear Poisson- Boltzmann Equation*, The Journal of Physical Chemistry B, 114(31):10114-10125,2010.
- [17] X. Zhang, JP. Hsu, ZS. Chen, LH. Hsien, MH. Ku and S. Tseng, *Electrophoresis of a charge-regulated soft sphere in a charged cylindrical pore*, The Journal of Physical Chemistry B, 114(4):1621-1631,2010.
- [18] KL. Liu, JP. Hsu, and S. Tseng *Influence of membrane layer properties on the electrophoretic behavior of a soft particle*, Electrophoresis, 32(21):3053-3061,2011.
- [19] LH. Yeh, KY. Feng, JP. Hsu and S. Tseng, *Influence of boundary on the effect of double-layer polarization and the electrophoretic behavior of soft biocolloids*, Colloids and Surfaces B: Biointerfaces, 88(2):559-567,2011.
- [20] CH. Chou, JP. Hsu, CC. Kuo, H. Ohshima, S. Tseng, and RM. Wu, *Importance of the porous structure of a soft particle on its electrophoretic behavior*, Colloids and Surfaces B: Biointerfaces, 93(41):154-160,2012.
- [21] S. Tseng, JP. Hsu, HM. Lo, and LH. Yeh, *Electrophoresis of a soft sphere in a necked cylindrical nanopore*, Physical Chemistry Chemical Physics, 15(28):11758-11765,2013.
- [22] AC. Barbatí, and BJ. Kirby, *Soft diffuse interfaces in electrokinetics—theory and experiment for transport in charged diffuse layers*, Soft Matter, 8(41):10598-10613,2012.
- [23] S. Raafatnia, O. Hickey, and C. Holm *Mobility reversal of polyelectrolyte-grafted colloids in monovalent salt solutions*, Physical review letters, 113(24):238301,2014.
- [24] S. Bhattacharyya, and S. De *Influence of rigid core permittivity and double layer polarization on the electrophoresis of a soft particle: A numerical study*, Physics of Fluids (1994-present), 28(1):012001,2016.
- [25] S. De, S. Bhattacharyya, and PP. Gopmandal *Importance of core electrostatic properties on the electrophoresis of a soft particle*, Physical Review E (1994-present), 94(2):022611,2016.
- [26] M. Moussa, C. Caillet, R. M. Town, and JFL. Duval, *Remarkable electrokinetic features of charge-stratified soft nanoparticles: Mobility reversal in monovalent aqueous electrolyte*, Langmuir, 31(20):5656-5666,2015.